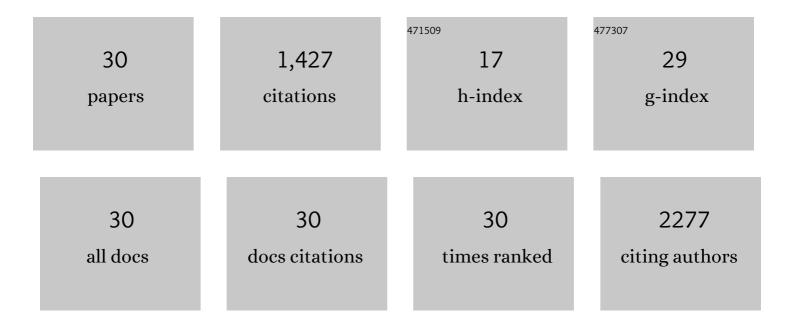
Siamak P Nejad-Davarani

List of Publications by Year in descending order

Source: https://exaly.com/author-pdf/3552156/publications.pdf Version: 2024-02-01



#	Article	IF	CITATIONS
1	Impairments of white matter tracts and connectivity alterations in five cognitive networks of patients with multiple sclerosis. Clinical Neurology and Neurosurgery, 2021, 201, 106424.	1.4	1
2	Performance of deep learning synthetic CTs for MRâ€only brain radiation therapy. Journal of Applied Clinical Medical Physics, 2021, 22, 308-317.	1.9	15
3	Quantification of brain cholinergic denervation in dementia with Lewy bodies using PET imaging with [18F]-FEOBV. Molecular Psychiatry, 2019, 24, 322-327.	7.9	37
4	Large field of view distortion assessment in a lowâ€field MR â€linac. Medical Physics, 2019, 46, 2347-2355.	3.0	21
5	Geometric and dosimetric impact of anatomical changes for <scp>MR</scp> â€only radiation therapy for the prostate. Journal of Applied Clinical Medical Physics, 2019, 20, 10-17.	1.9	19
6	Generating synthetic CTs from magnetic resonance images using generative adversarial networks. Medical Physics, 2018, 45, 3627-3636.	3.0	207
7	Diffusion-Derived Magnetic Resonance Imaging Measures of Longitudinal Microstructural Remodeling Induced by Marrow Stromal Cell Therapy after Traumatic Brain Injury. Journal of Neurotrauma, 2017, 34, 182-191.	3.4	9
8	A parametric model of the brain vascular system for estimation of the arterial input function (AIF) at the tissue level. NMR in Biomedicine, 2017, 30, e3695.	2.8	15
9	An extended vascular model for less biased estimation of permeability parameters in DCEâ€₹1 images. NMR in Biomedicine, 2017, 30, e3698.	2.8	12
10	Optimization of a novel large field of view distortion phantom for MRâ€only treatment planning. Journal of Applied Clinical Medical Physics, 2017, 18, 51-61.	1.9	20
11	Cell Treatment for Stroke in Type Two Diabetic Rats Improves Vascular Permeability Measured by MRI. PLoS ONE, 2016, 11, e0149147.	2.5	11
12	Resting state fMRI connectivity analysis as a tool for detection of abnormalities in five different cognitive networks of the brain in MS patients. Clinical Case Reports and Reviews, 2016, 2, 464-471.	0.1	10
13	NIMG-50SURVIVAL RATE PREDICTION IN PATIENTS WITH GLIOBLASTOMA MULTIFORME (GBM), USING DYNAMIC CONTRAST ENHANCED MRI AND NESTED MODEL SELECTION TECHNIQUE (NMS). Neuro-Oncology, 2015, 17, v165.2-v165.	1.2	0
14	Measurement of rat brain tumor kinetics using an intravascular MR contrast agent and DCEâ€MRI nested model selection. Journal of Magnetic Resonance Imaging, 2014, 40, 1223-1229.	3.4	15
15	Stroke Increases Neural Stem Cells and Angiogenesis in the Neurogenic Niche of the Adult Mouse. PLoS ONE, 2014, 9, e113972.	2.5	80
16	Perfusion and Diffusion Abnormalities of Multiple Sclerosis Lesions and Relevance of Classified Lesions to Disease Status. Journal of Neurology & Neurophysiology, 2013, s12, 12.	0.1	6
17	Comparison of Neurite Density Measured by MRI and Histology after TBI. PLoS ONE, 2013, 8, e63511.	2.5	19
18	MRI of Neuronal Recovery after Low-Dose Methamphetamine Treatment of Traumatic Brain Injury in Rats. PLoS ONE, 2013, 8, e61241.	2.5	17

#	Article	IF	CITATIONS
19	Characterizing Brain Structures and Remodeling after TBI Based on Information Content, Diffusion Entropy. PLoS ONE, 2013, 8, e76343.	2.5	19
20	MRI Measurement of Angiogenesis and the Therapeutic Effect of Acute Marrow Stromal Cell Administration on Traumatic Brain Injury. Journal of Cerebral Blood Flow and Metabolism, 2012, 32, 2023-2032.	4.3	23
21	Blood-Brain-Barrier Imaging in Brain Tumors: Concepts and Methods. Neurographics, 2012, 2, 48-59.	0.1	9
22	MRI Detects Brain Reorganization after Human Umbilical Tissue-Derived Cells (hUTC) Treatment of Stroke in Rat. PLoS ONE, 2012, 7, e42845.	2.5	27
23	Model selection for DCEâ€₹1 studies in glioblastoma. Magnetic Resonance in Medicine, 2012, 68, 241-251.	3.0	74
24	Ascl1 Lineage Cells Contribute to Ischemia-Induced Neurogenesis and Oligodendrogenesis. Journal of Cerebral Blood Flow and Metabolism, 2011, 31, 614-625.	4.3	78
25	Increasing tPA Activity in Astrocytes Induced by Multipotent Mesenchymal Stromal Cells Facilitate Neurite Outgrowth after Stroke in the Mouse. PLoS ONE, 2010, 5, e9027.	2.5	94
26	Patterns and Dynamics of Subventricular Zone Neuroblast Migration in the Ischemic Striatum of the Adult Mouse. Journal of Cerebral Blood Flow and Metabolism, 2009, 29, 1240-1250.	4.3	108
27	Magnetic Resonance Imaging Investigation of Axonal Remodeling and Angiogenesis after Embolic Stroke in Sildenafil-Treated Rats. Journal of Cerebral Blood Flow and Metabolism, 2008, 28, 1440-1448.	4.3	133
28	Augmented Healing Process in Female Mice with Acute Myocardial Infarction. Gender Medicine, 2007, 4, 230-247.	1.4	27
29	Investigation of neural progenitor cell induced angiogenesis after embolic stroke in rat using MRI. NeuroImage, 2005, 28, 698-707.	4.2	151
30	Comparison of multiwavelet, wavelet, Haralick, and shape features for microcalcification classification in mammograms. Pattern Recognition, 2004, 37, 1973-1986.	8.1	170